Supporting Information

Oxidative stress induced by pure and iron-doped amorphous silica nanoparticles in sub-toxic conditions

Running title: **Oxidative stress and cytotoxicity of amorphous nanosilica**

Dorota Napierska[†], Virginie Rabolli[‡], Leen C.J. Thomassen[§], David Dinsdale[‖], Catherine Princen[‡], Laetitia Gonzalez[¶], Katrien L.C. Poels[⊥], Micheline Kirsch-Volders[¶], Dominique Lison[‡], Johan A. Martens[§] and Peter H. Hoet[†]*

[†]Unit for Lung Toxicology, Katholieke Universiteit Leuven, Herestraat 49, O&N1-706, 3000 Leuven, Belgium

[‡]Industrial Toxicology and Occupational Medicine unit, Universite´ Catholique de Louvain, 1200 Brussels, Belgium

[§]Center for Surface Chemistry and Catalysis, Katholieke Universiteit Leuven, 3001 Heverlee, Belgium

[‖]MRC Toxicology Unit, Lancaster Road, Leicester LE1 9HN, UK

[¶]Laboratory of Cell Genetics, Vrije Universiteit Brussel, 1050 Brussels, Belgium

[⊥]Laboratory for Occupational Hygiene and Toxicology, Katholieke Universiteit Leuven, 3000 Leuven, Belgium

*To whom correspondence should be addressed. Unit for Lung Toxicology, Katholieke Universiteit Leuven, Herestraat 49, O&N1-706, 3000 Leuven, Belgium.

Tel. +32 16330197, Fax: +32 16 330806

E-mail: peter.hoet@med.kuleuven.be

METHODS

Additional silica nanoparticles characterization

Electron microscopy images of the nanoparticles and corresponding scale bars are shown in Figure S1. S-16 and SFe were analyzed by transmission electron microscopy. S-60 was analyzed by scanning electron microscopy (Figure S1). The particles show a narrow size distribution and a spherical morphology. The average particle size and standard deviation are given in Table 1. The surface structure of the nanoparticles was analyzed by nitrogen sorption and small angle X-ray scattering (SAXS) techniques. Nitrogen sorption showed a high BET surface area for the small S-16 and SFe nanoparticles. The discrepancy between BET and external surface area in all samples and the considerable micropore volume, detected in the smallest nanoparticles, point towards rough surface areas. The external surface area of all samples corresponds well to the surface area based on the average TEM diameter.[1]

SAXS measurements were performed on SAXSess mc2 instrument (Anton Paar, Graz, Austria) with line-collimated CuKα radiation. SAXS patterns of sample suspensions placed in a 1 mm vacuum-tight quartz capillary were recorded at RT. Normalization; background subtraction and desmearing was done in the SAXSquant software (Anton Paar). Model fits were performed by using the NIST SANS package for Igor Pro software (Wavemetrics).[2] SAXS measurements confirmed the diameter of the nanoparticles measured by electron microscopy. Furthermore, the surface structure of the particles was analyzed. The SAXS patterns of the S-60 nanoparticles was fitted with the Guinier-Porod model,[3] yielding a Porod slope of 3.37, indicating that these nanoparticles are surface fractals with a rough particle surface (cfr. TEM Figure S1).[4] The smaller nanoparticles S16 and SFe were fitted with a raspberry model.[5] This model assumes a rough particle surface. The model parameters showed that the surface consisted of ca. 2 nm particles which were aggregated during the synthesis procedure,[6] yielding surface fractals. In conclusion, SAXS as well as nitrogen

sorption and EM techniques indicate a considerable surface roughness for all particles.

To investigate the chemical nature of the nanoparticles, their atomic composition was determined by inductively coupled plasma (ICP) spectroscopy after dissolving the nanoparticles. The concentration of silicon in the samples was determined by ICP-atomic emission spectroscopy and presented in mass and molar concentration in Table S1. The mass and molar concentration of iron was determined by ICP- mass spectroscopy (Table S1). The iron doped nanoparticles contained about 200 times more iron than the silica samples which were synthesized without addition of iron. The traces of iron in the S-16 and S-60 samples are likely to originate from impurities in the chemicals used in the synthesis procedure. The presence of iron, available for cells (soluble or present on the particle surface), was investigated qualitatively via a complexation reaction with potassion isothiocyantate. A reddish color, showing the presence of iron was only detected in the SFe sample. The intensity of the color was too low for a quantitative determination.

The size of the nanoparticles in suspension was analyzed by dynamic light scattering. The size of the nanoparticles in the mother liquor (ethanol) did not change upon dialysis (data not shown). The stability of the aqueous nanoparticles suspensions for over 4 years was confirmed by repeated DLS measurements (Figure S2, black lines). For cellular experiments, DLS measurements were performed in DMEM. Therefore, the stability of the particles was analyzed in this cell culture medium. Upon suspending the particles in the DMEM medium, the hydrodynamic particles size distribution of the nanoparticles barely changed with respect to the particle size distribution in water (Figure S2, grey lines). The particles were stable for over 72h in DMEM. The stability of the particles is granted over the time span of the (a)-cellular experiments in physiological media.

Zeta potential analysis was performed on a BIC 90 Plus instrument (Brookhaven). The electrophoretic mobility was determined by phase analysis of the scattered laser light in forward

scattering mode (angle 15°). The average zeta potential of the particles was calculated over 10 runs. The sample preparation and measurements were described in detail previously (ref thomassen). The large negative surface charge of the silica particles in water (with 1 mM KCl for conductivity), ensured the stability of the particles based on electrostatic repulsions, as confirmed by DLS (Table S1). In DMEM cell culture medium, the surface charge of the particles is lowered, indicating a limited stability of the nanoparticles in this medium (more than 72 h according to DLS measurements).[1]

RESULTS

Table S1. Concentration of silicon and iron in the samples determined by ICP-AES and ICP-MS respectively

	S-16	S-60	SFe
Size (EM, nm)	16.4 ± 2.5	60.4 ± 8.3	16.1 ± 1.9
Concentration Si (mg/ml)	1.51	2.16	1.04
Concentration SiO_2 (mg/ml)	3.24	4.63	2.23
Concentration Fe (µg/ml)	0.017	0.011	0.254
Molar concentration Si or SiO_2 (M)	0.0539	0.0771	0.0372
Molar concentration Fe (µM)	0.3	0.2	4.54
BET surface area (m^2/g)	220	42	392
External surface area (m^2/g)	183	33	254
Micropore volume (m^2/g)	22	0	28
Zeta potential in 1 mM KCl (mV)	-67	-24	-18
Zeta potential in DMEM (mV)	-13	-13	-14

Table S2. Viability of EA.hy926 cells pre-incubated overnight with 5 mM NAC and exposed to t*ert*-butyl hydroperoxide (TBHP) and toxic dose of silica nanoparticles. Results are presented as a percentage of the control values. Values are mean ± SD of two independent experiments. **p*<0.05, ***p*<0.01 vs. control

		1 h	2h	4h	6h	24h
TBHP	0.5 µM	94 ± 5		86 ± 4		
S16	40 µg/ml		88 ± 3		61 ± 8*	52 ± 6**
	50 µg/ml	97 ± 4		79 ± 9*		
S60	250 µg/ml	93 ± 7	84 ± 11	69 ± 6**	70± 17*	42 ± 13**
SFe	40 µg/ml		91 ± 9		61 ± 14**	51 ± 16**
	50 µg/ml	92 ± 6		63 ± 11**		

Table S3. Heme oxygenase-1 (HO-1) gene expression in EA.hy926 cells pre-incubated overnight with 5 mM NAC and exposed to toxic doses of SiO_2-NPs. Results are presented as fold change over control. Values are mean ± SD of two independent experiments. *p<0.05, **p<0.01 vs. control

		HO-1 fold change over ctrl
2h	S16 (40 µg/ml)	1.1 ± 0.2
	S60 (250 µg/ml)	1.1 ± 0.2
	SFe (40 µg/ml)	1.2 ± 0.1
6h	S16 (40 µg/ml)	5.1 ± 1.2**
	S60 (250 µg/ml)	7.2 ± 2.2**
	SFe (40 µg/ml)	2.7 ± 0.5*
24h	S16 (40 µg/ml)	1.8± 0.4**
	S60 (250 µg/ml)	2.3 ± 0.3**
	SFe (40 µg/ml)	2.2 ± 0.2**

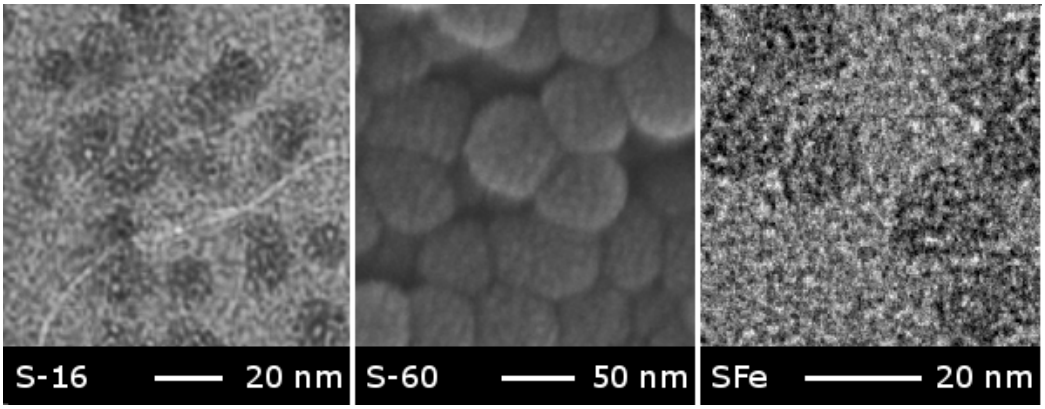

Figure S1. TEM images of S-16 and SFe, and SEM image of S-60

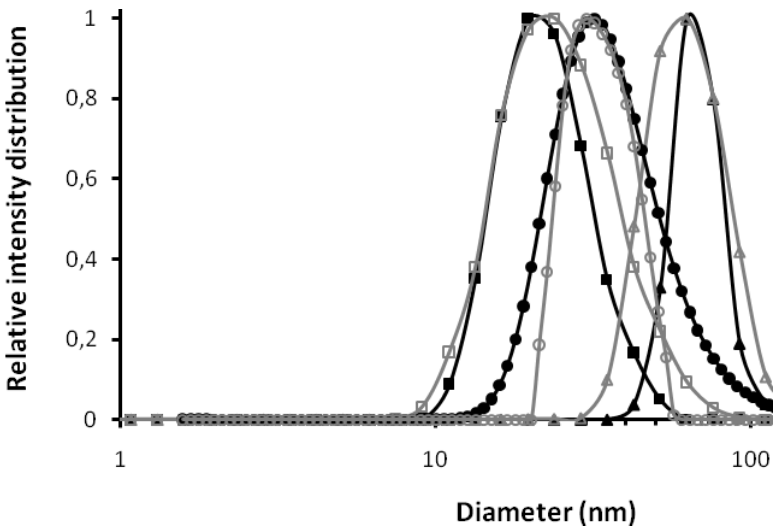

Figure S2. Hydrodynamic particle size distribution of the nanoparticles (S-16: squares, S-60: triangles and SFe: circles), in water (black line, full symbols) and in DMEM (grey line, open symbols)

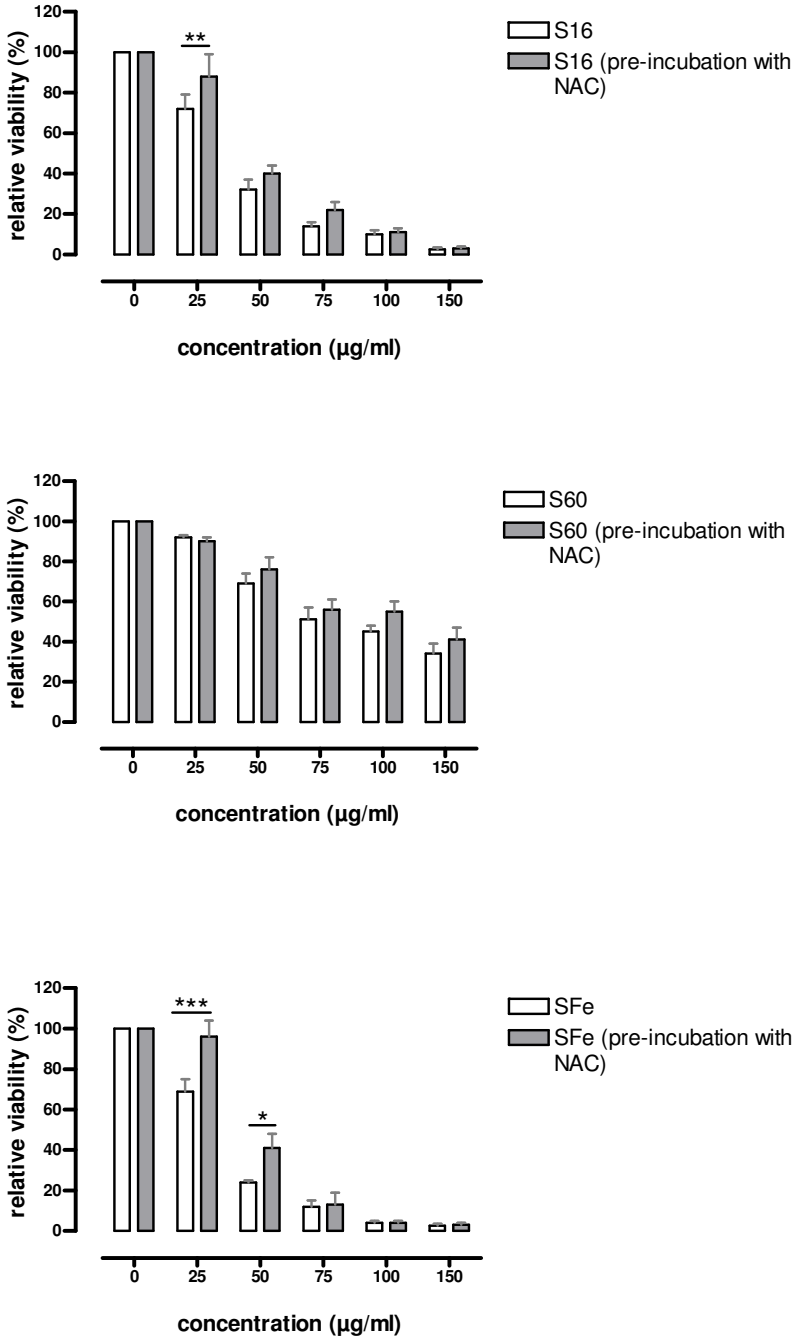

Figure S3. The influence of the antioxidant *N*-acetylcysteine (NAC) on the cytotoxic activity (LDH release) of SiO_2-NPs. Endothelial cells were pre-incubated overnight with 5 mM NAC and exposed to SiO_2-NPs for 24 h. Results are presented as a percentage of the control values. Values are mean ± SD of three independent experiments. *p<0.05; **p<0.01; ***p<0.001

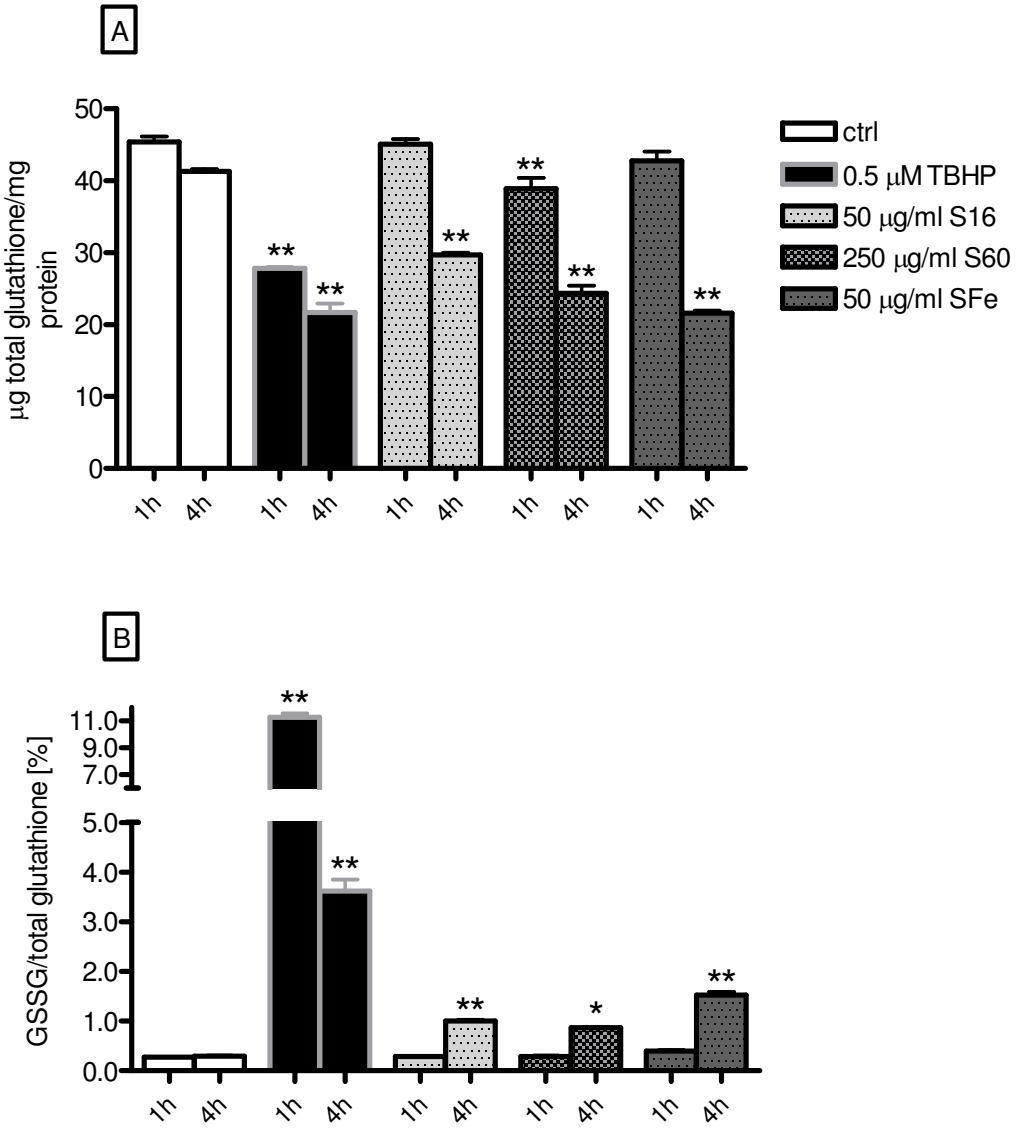

Figure S4. The influence of the antioxidant *N*-acetylcysteine (NAC) on intracellular glutathione levels in EA.hy926 cells exposed to SiO_2-NPs. Cells were pre-incubated overnight with 5 mM NAC and exposed to toxic doses of nanosilica. (A) total intracellular glutathione (GSSG and GSH), and (B) ratio of oxidized (GSSG) to total intracellular glutathione content in EA.hy926 cells. Glutathione levels are normalized to protein content. Values are mean ± SD of two independent experiments. *p<0.05; **p<0.01 vs. control.

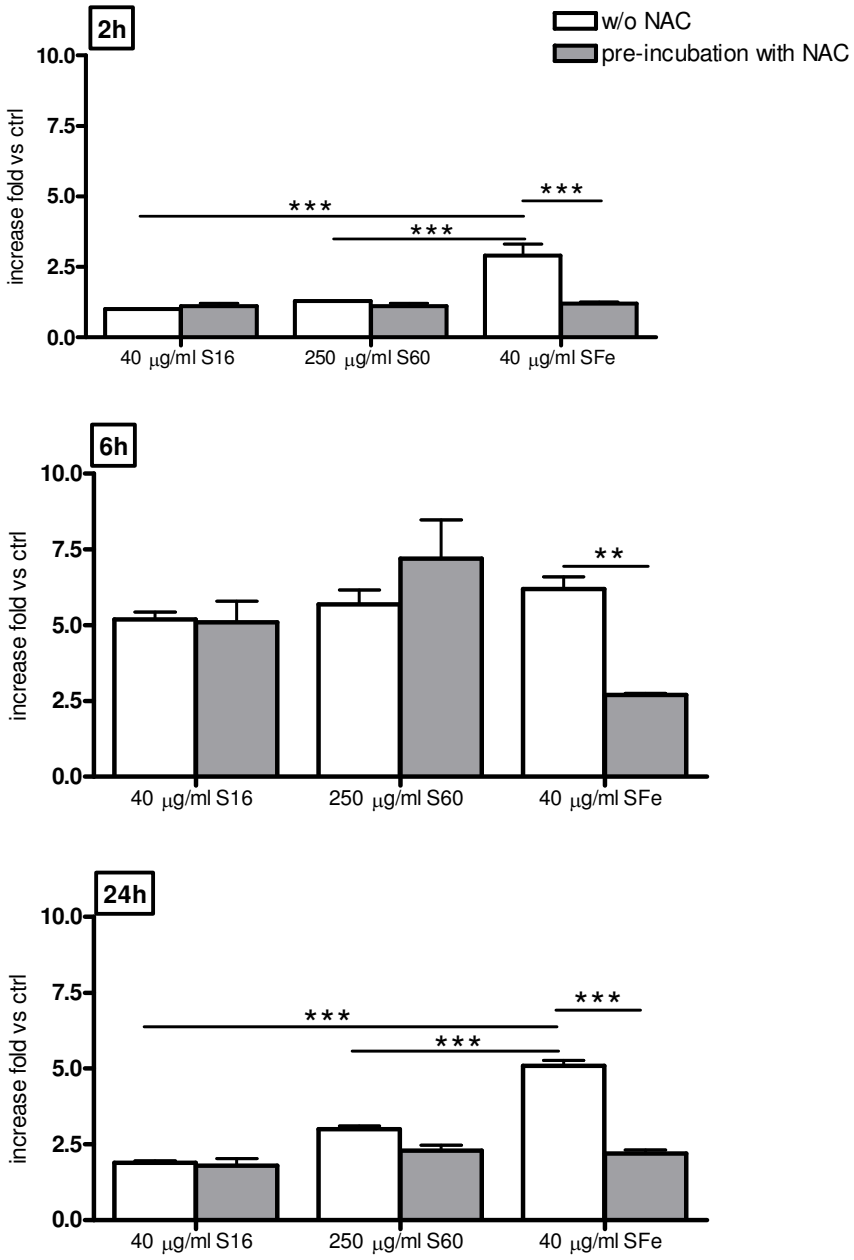

Figure S5. The influence of the antioxidant *N*-acetylcysteine (NAC) on heme oxygenase-1 (HO-1) gene expression in EA.hy926. Cells were or not pre-incubated overnight with 5 mM NAC and exposed to toxic doses of SiO_2-NPs. Results are presented as fold change over control. Values are mean ± SD of two independent experiments. $^{**}p<0.01$; $^{***}p<0.001$

REFERENCES

(1) Thomassen, L. C., Aerts, A., Rabolli, V., Lison, D., Gonzalez, L., Kirsch-Volders, M., Napierska, D., Hoet, P. H., Kirschhock, C. E., and Martens, J. A. (2010) Synthesis and characterization of stable monodisperse silica nanoparticle sols for in vitro cytotoxicity testing. *Langmuir 26*, 328-335.

(2) Kline, S. (2006) Reduction and analysis of SANS and USANS data using IGOR Pro. *J. Appl. Crystallogr. 39*, 895-900.

(3) Hammouda, B. (2010) A new Guinier–Porod model. *J. Appl. Crystallogr. 43*, 716-719.

(4) Brinker, C.J., Scherer, G.W. (1990) Sol-gel science: the physics and chemistry of sol-gel processing. Academic Press Inc., San Diego, CA. 908 p.

(5) Larson-Smith, K., Jackson, A., Pozzo, D.C. (2010) Small angle scattering model for Pickering emulsions and raspberry particles. *J. Colloid. Interface Sci. 343*, 36-41.

(6) Iler, R.K. (1981) The Surface Chemistry of Amorphous Synthetic Silica: Interaction with Organic Molecules in an Aqueous Medium, in Health Effects of Synthetic Silica Particulates (Dunnom, D. D., Ed.) pp 3-21, American Society for Testing and Materials, Philadelphia, PA.